

Early and delayed stages in the solubilization of purple membrane by a polyoxyethylenic surfactant

Ana-Rosa Viguera, Juan-Manuel González-Mañas, Stefka Taneva¹, Félix M. Goñi^{*}

Department of Biochemistry, University of the Basque Country, P.O. Box 644, 48080 Bilbao, Spain

Received 25 March 1994; revised 19 July 1994

Abstract

The purpose of this paper is to explore the reasons by which purple membrane solubilization by detergents takes hours, or even days, to reach equilibrium, while most biomembranes are solubilized in a matter of seconds, or minutes. With that aim, changes in the purple membrane absorption spectrum produced by hydrogenated Triton X-100 under equilibrium conditions (24 h) have been compared to those caused by the same surfactant in the minute, second and sub-second time scale. It is found that the various processes that accompany, or lead to, solubilization are already detected, and even reach an apparent equilibrium, in the 10 s that follow detergent addition. No new phenomena are detected in the following minutes, or hours, that are relevant to the process under study. This leads to the conclusion that the long solubilization process consists of the repeated operation of simple phenomena that are relatively fast in themselves. A hypothesis is proposed according to which the tight crystalline organization of the purple membrane prevents the insertion of detergent monomers in the lipid bilayer; instead, the surfactant would bind the periphery of the patches, i.e., the hydrocarbon-water contact region, and solubilization would take place gradually, from the periphery towards the core of the membrane patches, at a progressively lower rate as the amounts of free detergent and detergent-binding sites are decreased by the previous solubilization steps.

Keywords: Membrane solubilization; Purple membrane; Surfactant

1. Introduction

Purple membrane has often been used as a biological model in studies on membrane-surfactant interactions. These are important in view of our limited knowledge of the mechanisms involved in the solubilization and functional reconstitution of membrane systems. The work by Reynolds and Stoerkenius [1], Dencher and Heyn [2], Casadio et al. [3], London and Khorana [4], or Lam and Packer [5] established the grounds of our present knowledge in this field. The reconstitution of bacteriorhodopsin into phospholipid bilayers, starting from detergent-solubilized protein, was studied in detail by Rigaud et al. [6]. More recently, the 'effective' (as defined by Lichtenberg et al. [7]) detergent/protein ratios for purple membrane solubilization by Triton X-100 have been established [8]. Our

own contribution to this field [9–12] has intended to correlate data on the solubilization of membrane components with those on spectral shifts and light-dark adaptation, by a combination of biochemical and spectroscopic data.

One aspect that has not received much attention up to now is the kinetics of the process. Dencher and Heyn [2] and Casadio et al. [3] already noted that, after Triton X-100 addition, equilibrium takes hours, or even days, to be reached, instead of seconds, or minutes, as in most biomembranes. In spite of that, kinetic studies are virtually non-existent. The data in the present paper are intended to fill this gap: our results show that, from the millisecond range, a number of processes occur that will, eventually, lead to the observed equilibrium effects. Triton X-100 had been used in many of the previous studies; in our case, hydrogenated (or reduced) Triton X-100 (RTX) has been preferred, since its solubilizing properties are very similar to those of the parent compound [12], while some disadvantageous properties of Triton X-100 (e.g., chemical heterogeneity, fluorescence, presence of oxidation products) are greatly diminished [13,14].

Abbreviations: RTX, hydrogenated Triton X-100.

^{*} Corresponding author. Fax: +34 4 4648500.

¹ Permanent address: Central Laboratory of Biophysics, Bulgarian Academy of Sciences, Sofia 1113, Bulgaria.

2. Materials and methods

Hydrogenated Triton X-100 (RTX), also called 'reduced Triton X-100', was supplied by Aldrich Chemie (Steinheim, Germany). Egg phosphatidylcholine was from Lipid Products (South Nutfield, UK). *Halobacterium halobium* S9 was grown and purple membrane purified according to Oesterhelt and Stoekenius [15]. Membranes were resuspended in a 20 mM Tris-HCl, 20 mM maleate, pH 7.0 buffer, at a concentration of 0.6 mg protein/ml. Membrane suspensions were mixed with equal volumes of the appropriate surfactant solutions, in the same buffer, to give the desired detergent/protein ratios [16]. Light-adapted membrane was used in all the experiments; detergent treatments took place under illumination ($30 \mu\text{mol einstein s}^{-1} \text{ cm}^{-1}$).

Absorption spectra were recorded in a Uvikon 860 Kontron spectrophotometer. Scan rates varied between 100 and 500 nm/min. Quartz cuvettes (1 cm pathlength) were used. The data were digitized and processed with a Kontron computer (CPV 8088 + data processor 8087).

For stopped-flow measurements, a Hi-Tech spectrometer was used, consisting of the following elements: SF-51 sample handling unit, Osram XBO-150W xenon lamp, MG-10 monochromator, PM-60 photomultiplier, connected to a SU-40 amplifier. At least six transients were averaged for each measurement. The optical path for absorbance measurements was 1 cm. The signal was transferred through an A/D converter to an Apple IIe computer, through which the machine was operated. Data were processed in a PC computer. Curves were fitted to exponential equations using a Gauss-Newton algorithm. The curves (as shown in Fig. 3) were fitted to single or double first-order exponentials, or to a single second-order function. The best fit (residuals within $\pm 3\%$ of experimental values) was found to be a single first-order exponential. Fast spectral scanning took place by means of an MG 3000 spinning monochromator (Hi-Tech, Salisbury, UK) that allows recording of one spectrum every 95 ms; each spectrum (350–800 nm) is recorded in 7.2 ms. Absorption band maxima are calculated by means of an interpolation algorithm [17]. The dead time of the stopped-flow system was of 2.3 ms, after measurements with 2-dichlorodiphenol + ascorbate. The contents of the syringes, loaded respectively with detergent and purple membrane suspensions, were mixed in a 1:1 ratio.

Quasi-elastic light-scattering measurements were performed in a Malvern Zetasizer 4.

3. Results

3.1. Equilibrium studies

Prior to recording the kinetic data, the effects of hydrogenated Triton X-100 (RTX) on the visible spectrum of

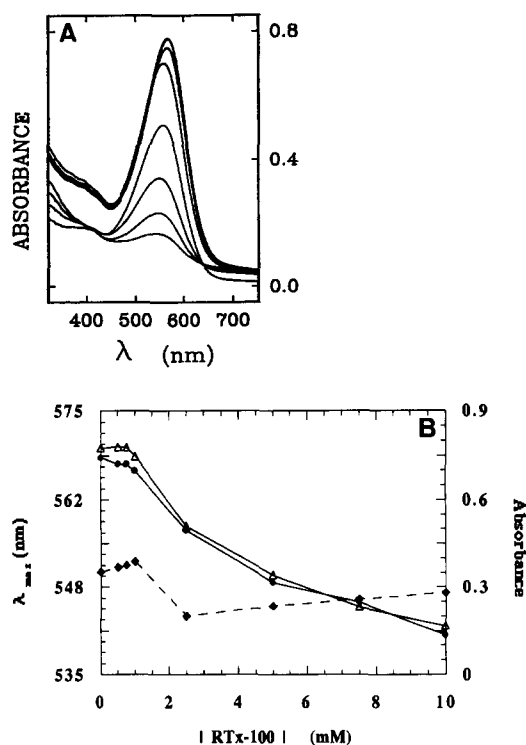


Fig. 1. The effects of hydrogenated Triton X-100 (RTX) on the purple membrane visible spectrum. (A) Spectra were recorded after 24 h incubation, in the presence of light, of purple membrane (0.6 mg ml^{-1}) with increasing surfactant concentrations (downwards in the figure: 0, 0.5, 0.75, 1, 2.5, 5, 7.5 and 10 mM). (B) Changes in spectral λ_{max} (●) and A_{350} (◆) and A_{587} (Δ), as a function of surfactant concentration.

purple membrane were examined under equilibrium conditions. Fig. 1A shows the spectra of different purple membrane-surfactant preparations, equilibrated for 24 h, under illumination. The overall effect consists of a decrease in turbidity (as apparent absorbance in the 350–400 nm region), a blue shift of λ_{max} , and a decrease in the intensity of the absorption band (Fig. 1B). These changes are more remarkable at surfactant concentrations above 2 mM. All these data confirm the similarity between RTX and Triton X-100 spectral effects [9,10].

Equilibrium measurements were also carried out, by quasi-elastic light-scattering, of the decrease in size of purple membrane patches when treated with increasing concentrations of Triton X-100. The results in Fig. 2 show that the average size of the patches decreases gradually with increasing surfactant concentrations; in addition, when the supernatants of detergent-treated purple membrane suspensions are examined, the solubilized particles are of a constant size, which is the same as attained by the whole membrane suspension when treated with the highest tested (10 mM) detergent concentrations.

3.2. Kinetic studies. The first seconds

Observation of early surfactant effects required the use of stopped-flow techniques. In a first series of experi-

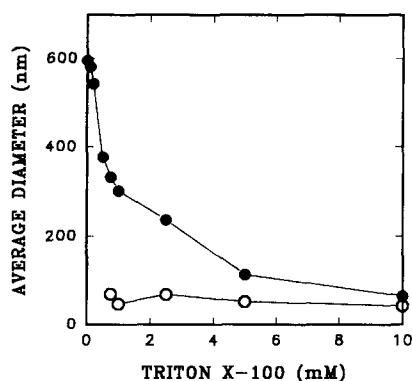


Fig. 2. Equilibrium measurements of the average diameter of membranous systems in the presence of increasing concentrations of Triton X-100. Average diameters (in nm) were estimated by quasi-elastic light-scattering. Membrane suspensions were left to equilibrate with the detergent for 24 h. Purple membrane (●), and purple membrane supernatants ($100\,000\times g$, 4°C , 2 h) (○), after detergent treatments.

ments, fixed wavelengths were used: 350 nm, for observing changes in turbidity, and 587 nm, at which changes in the absorbance of the retinal chromophore are maximal (Fig. 1). The transients recorded at 350 and 587 nm for a variety of RTX concentrations are shown in Fig. 3. According to these data, two main detectable phenomena occur in the first seconds of purple membrane-RTX interaction, namely: (i) a decrease in turbidity (A_{350}), that is virtually completed within the first 50 ms, except for the lowest RTX concentrations tested (Fig. 3D,E). The same phenomenon is reflected, at a correspondingly smaller scale, as a decrease in A_{587} , particularly for the membrane-solubilizing surfactant concentrations (> 1 mM) (Fig. 3A,B). This effect is preceded by an increase in turbidity, occurring mainly during the instrumental dead

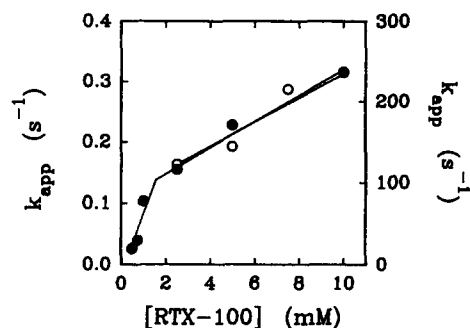


Fig. 4. Apparent rate constants for the early spectral changes in absorption and turbidity (A_{350}). Values of k_{app} for the variations in A_{587} (○) and A_{350} (●) are plotted as a function of surfactant concentration.

time, 2.3 ms, and whose origin cannot be explained at present (Fig. 3D). (ii) A marked decrease in A_{587} , taking place along the first 10 s (Fig. 3C). The specific effect on A_{587} (Fig. 3C) is only detected within the solubilizing range of surfactant concentrations (≥ 2.5 mM).

Both the process detected at 350 nm (in the 50 ms scale, Fig. 3D) and the slower one observed at 587 nm (in the scale of seconds, Fig. 3C) can be fitted to single exponential curves, suggesting a first-order process for the membrane. The corresponding apparent rate constants (k_{app}) are plotted in Fig. 4 as a function of RTX concentration. The apparent rate constants for the decrease in turbidity can be adjusted to two straight lines, whose intersection corresponds to the frontier between solubilizing and non-solubilizing surfactant concentrations. The linear increase in apparent rate constants with surfactant concentration indicate also a first-order process for the detergent. Thus, the decrease in turbidity appears to occur as a result of direct membrane-surfactant interaction, perhaps represent-

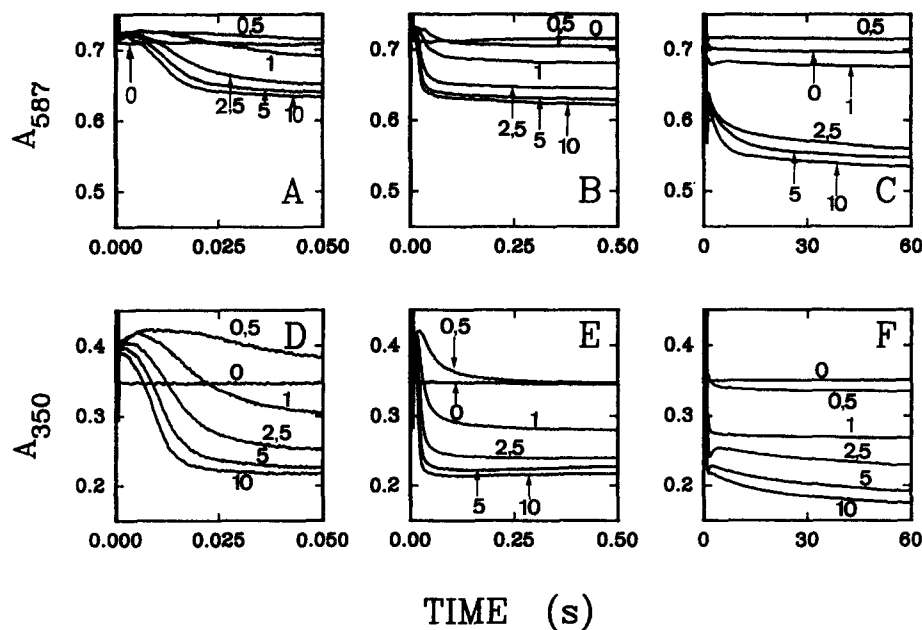


Fig. 3. The kinetics of early RTX effects on the purple membrane absorption and turbidity. Changes in absorption are followed as changes in A_{587} in panels A–C. Changes in turbidity are followed as changes in A_{350} in panels D–F. Surfactant concentrations were: 0, 0.5, 1, 2.5, 5 and 10 mM.

ing the binding of RTX to the periphery of purple membrane sheets (see Discussion). The corresponding k_{app} values for the slow process of chromophore bleaching (decrease of A_{587}) may also be adjusted to a straight line (Fig. 4). When the maximal amplitudes of the exponential curves are plotted as a function of detergent concentration (not shown) they run in parallel with the corresponding k_{app} values. Thus, the amplitudes and rate constants of the changes in turbidity and absorbance occurring in the first seconds after surfactant addition increase linearly with RTX concentration, a discontinuity marking the minimum solubilizing concentration.

In a different set of measurements, a fast scanning device (Spectrascan, Hi-Tech) was used to record whole spectra (350–800 nm) in the first seconds of membrane-surfactant interaction. The results are summarized in Fig. 5, revealing an additional surfactant effect, namely a blue-shift of the absorption maximum. This is only seen at solubilizing RTX concentrations, and reaches apparent completion in about 10 s, suggesting that it is part of the same effect detected as a decrease in A_{587} . This decrease in absorbance is partly due to the blue-shift of the main absorption band (Fig. 5); in turn, the latter is most probably attributed to retinal isomerization, from *all-trans* to 13-*cis*, i.e., the same kind of isomerization occurring after purple membrane dark adaptation. Equilibrium measurements have shown the surfactant-dependent isomerization of retinal [3,9–11]. This process starts, and appears to reach an equilibrium, at an early stage.

3.3. Kinetic studies. The first minutes

Conventional absorption spectra were recorded every 3 min, on each detergent-treated membrane suspension, for half-an-hour. The gradual surfactant effects are best appreciated in difference spectra 'native minus detergent-treated membrane' computed for each spectrum in the time-course experiment. The results are summarized in Fig. 6; changes in both turbidity and retinal absorbance are detected, the

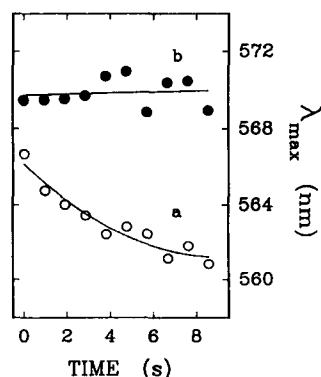


Fig. 5. Early effects of RTX on the purple membrane visible spectrum. λ_{max} of fast-recording spectra after addition of (○) 10 mM and (●) 0.5 mM RTX. The first spectrum was recorded 25 ms after surfactant addition; the interval between spectra was 0.95 s; the last spectrum was recorded after ≈ 8.5 s.

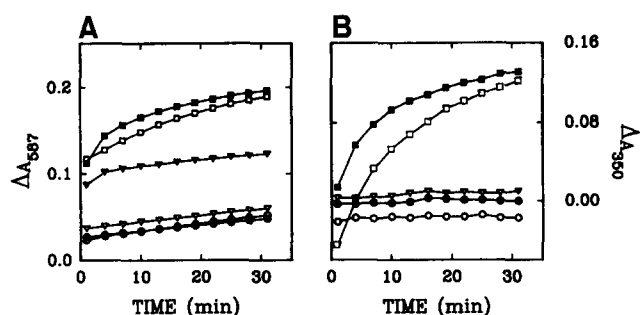


Fig. 6. Time-course of changes in absorbance after surfactant addition. (A) Changes in A_{587} ; (B) changes in A_{350} . Detergent concentrations were (○) 0.50, (●) 0.75, (▽) 1, (▼) 2.5, (□) 5, and (■) 10 mM.

latter involving a decrease in absorbance at 587 nm (i.e., $\Delta A > 0$). Low RTX concentrations appear to act steadily and slowly on this band, with only minor changes in turbidity, while, at higher concentrations, surfactant-induced changes in turbidity are large enough to perturb the absorbance of the retinal chromophore. This is clearly seen in Fig. 6A, where the decrease in absorption at 587 nm is plotted as a function of time. Linear plots are obtained for RTX concentrations up to 1 mM, while the 5 and 10 mM plots are clearly non-linear, and 2.5 mM constitutes a limiting case. It should be noted that, when turbidity changes do not perturb A_{587} measurements, the various straight lines show similar slopes, indicating that, in this range of time and RTX concentrations, the process does not depend on surfactant concentration. Fig. 6B shows, accordingly, that changes in turbidity (ΔA_{350}) are only detectable above 1 mM Triton.

The slow decrease in turbidity (Fig. 6B) is probably reflecting solubilization itself, i.e., the conversion of bilayer into micellar aggregates [8]; turbidity is known to decrease with all membrane solubilization processes, and, in the particular case of purple membrane, equilibrium measurements have shown a parallelism between turbidity decrease and solubilization [9]. The absorbance (A_{587}) changes (Fig. 6A) appear to be of the same nature than those seen in the first 10 s, now taking place at a much slower rate. This slow decrease in A_{587} occurs even at sub-lytic RTX concentrations; this phenomenon corresponds probably to the observation by Meyer et al. [8], under near-equilibrium conditions, of a change in λ_{max} at Triton X-100 concentrations not producing major changes in turbidity (i.e., their points a and a'). In summary, solubilization is a slow process reflected as a decrease in turbidity, occurs only above a given surfactant concentration, and is accompanied by other spectral effects (e.g., slow decrease in A_{587}) that occur at all surfactant concentrations.

4. Discussion

Previous time-resolved studies of membrane-surfactant interactions [18,19] have dealt with systems simpler than

purple membrane, i.e., liposomes. In the present case, purple membrane solubilization, leading ultimately to monomeric bacteriorhodopsin in detergent micelles [1], is a complex process, requiring hours to reach equilibrium [9]. Solubilization is accompanied by a decrease in turbidity, a decrease in A_{587} and a blue-shift of λ_{\max} . Although the process takes place over several hours, our data show that the detergent-induced spectral changes are already detected, and reach an apparent equilibrium, within the first seconds. Further steps of solubilization are not accompanied by any new phenomena that could be detected through changes in the highly sensitive bacteriorhodopsin absorption spectrum (apart from those due to imine bond hydrolysis, that appears to be a peripheral phenomenon in the solubilization process, with a half-time of the order of 1.5 h [20]). Instead, an increasing number of bacteriorhodopsin molecules appear to suffer the same structural changes observed in the first seconds, more and more molecules being slowly incorporated to the process.

Thus, the question arises on the reason for the very slow solubilization of purple membrane. The above data, together with the current knowledge of purple membrane structure, support a hypothesis according to which: (i) the crystalline structure of the purple membrane patches does not allow the incorporation of detergent monomers into the lipid bilayer, (ii) significant amounts of detergent can only bind the periphery of the patches, thus relieving the thermodynamically unfavourable hydrocarbon chain-water contacts, and (iii) solubilization starts at the periphery of the patches, and progresses gradually to reach the bacteriorhodopsin molecules in the centre of the patch. The process becomes slower with time, since less detergent and less detergent-binding sites remain available. In contrast, in other membranous systems, the detergent may partition into the whole of the lipid phase, and consequently solubilization occurs as an all-or-none, rather than a gradual, process. The hypothesis of a series of successive solubilization rounds, starting at the periphery of the patches, is supported by the results in the study, under equilibrium conditions, of detergent effects on the size of purple membrane patches shown in Fig. 2. Sodium cholate and similar detergents achieve an effective delipidation of the purple membrane, but no bacteriorhodopsin solubilization is produced; their mechanism of action appears to be very different from that of 'linear' surfactants such as RTX, as suggested previously [12].

González-Mañas et al. [9] asserted that Triton X-100 binds the purple membrane as fast as any other biomembrane. However, measurements of detergent binding in that study were carried out at sublytic surfactant concentrations (Triton X-100 < 1 mM). For that range of Triton and membrane concentrations, all detergent binding occurs at a very early stage; according to our hypothesis, the detergent would bind the periphery of the patches, but, the detergent/membrane ratio being sublytic, the process would end there. In the lytic concentration range, however, deter-

gent binding is gradual and slow, since the protein and lipid molecules at the centre of the patches can only bind substantial amounts of surfactant once the periphery has been converted into mixed micelles. It can be asserted, therefore, that the 'three-stage model' of membrane solubilization, proposed by Helenius and Simons [21], applies to purple membrane although the rate-limiting stage I (detergent binding) may present peculiarities in mechanism and kinetics.

Acknowledgements

S.T. thanks NATO for a post-doctoral studentship. This work was supported in part by grant No. PB88-0301 from DGICYT and grant No. 042.310-E033/90 from the University of the Basque Country.

References

- [1] Reynolds, J. and Stoeckenius, W. (1977) *Proc. Natl. Acad. Sci. USA* 74, 2803–2804.
- [2] Dencher, N.A. and Heyn, M.P. (1978) *FEBS Lett.* 96, 322–325.
- [3] Casadio, R., Gutowitz, H., Mowery, P., Taylor, M. and Stoeckenius, W. (1980) *Biochim. Biophys. Acta* 590, 13–23.
- [4] London, E. and Khorana, H.G. (1982) *J. Biol. Chem.* 257, 7003–7011.
- [5] Lam, E. and Packer, L. (1983) *Arch. Biochem. Biophys.* 221, 557–564.
- [6] Rigaud, J.L., Paternostre, M.T. and Bluzat, A. (1988) *Biochemistry* 27, 2677–2688.
- [7] Lichtenberg, D., Robson, R.J. and Dennis, E.A. (1983) *Biochim. Biophys. Acta* 737, 285–304.
- [8] Meyer, O., Ollivon, M. and Paternostre, M.T. (1992) *FEBS Lett.* 305, 249–253.
- [9] González-Mañas, J.M., Virto, M.D., Gurtubay, J.I.G. and Goñi, F.M. (1990) *Eur. J. Biochem.* 188, 673–678.
- [10] González-Mañas, J.M., Montoya, G., Rodríguez-Fernández, C., Gurtubay, J.I.G. and Goñi, F.M. (1990) *Biochim. Biophys. Acta* 1019, 167–169.
- [11] González-Mañas, J.M., Goñi, F.M., Tribout, M. and Paredes, S. (1990) *Arch. Biochem. Biophys.* 282, 239–243.
- [12] del Río, E., González-Mañas, J.M., Gurtubay, J.I.G. and Goñi, F.M. (1991) *Arch. Biochem. Biophys.* 291, 300–306.
- [13] Tiller, G.E., Mueller, T.J., Dockter, M.E. and Struve, W.G. (1984) *Anal. Biochem.* 141, 262–266.
- [14] Rial, E., Muga, A., Valpuesta, J.M., Arondo, J.L.R. and Goñi, F.M. (1990) *Eur. J. Biochem.* 188, 83–89.
- [15] Oesterheld, D. and Stoeckenius, W. (1974) *Methods Enzymol.* 31A, 667–678.
- [16] Mayer, L.D., Hope, M.H. and Cullis, P.R. (1986) *Biochim. Biophys. Acta* 858, 161–168.
- [17] Moffat, D.G., Kauppinen, J.K., Cameron, D.G., Mantsch, H.H. and Jones, R.N. (1986) *Computer Programs for Infrared Spectroscopy*, NRCC Bulletin No. 18, Ottawa.
- [18] Alonso, A., Urbaneja, M.A., Goñi, F.M., Carmona, F.G., Cánovas, F.G. and Gómez-Fernández, J.C. (1987) *Biochim. Biophys. Acta* 902, 237–246.
- [19] Elamrani, K. and Blume, A. (1982) *Biochemistry* 21, 521–526.
- [20] Viguera, A.R., Villa, M.J. and Goñi, F.M. (1990) *J. Biol. Chem.* 265, 2527–2532.
- [21] Helenius, A. and Simons, K. (1975) *Biochim. Biophys. Acta* 415, 29–79.